Compositional dependence of structural and electronic properties of Cu_{2}ZnSn(S,Se)_{4} alloys for thin film solar cells

Shiyou Chen, Aron Walsh, Ji-Hui Yang, X. G. Gong, Lin Sun, Ping-Xiong Yang, Jun-Hao Chu, and Su-Huai Wei

Phys. Rev. B **83**, 125201 — Published 1 March 2011

DOI: 10.1103/PhysRevB.83.125201

Compositional dependence of structural and electronic properties of the $Cu_2ZnSn(S,Se)_4$ alloys for thin film solar cells

Shiyou Chen[1,2], Aron Walsh[3], Ji-Hui Yang[1], X. G. Gong[1], Lin Sun[2], Ping-Xiong Yang[2], Jun-Hao Chu[2], and Su-Huai Wei[4]

[1] *Laboratory for Computational Physical Sciences and Surface Physics Laboratory, Fudan University, Shanghai 200433, China*
[2] *Laboratory of Polar Materials and Devices, East China Normal University, Shanghai 200241, China*
[3] *Department of Chemistry, University College London, London WC1E 6BT, UK and*
[4] *National Renewable Energy Laboratory, Golden, CO 80401, USA*

(Dated: January 13, 2011)

A thin-film solar cell based on $Cu_2ZnSn(S,Se)_4$ (CZTSSe) alloy was recently found to exhibit a light to electricity conversion efficiency of 10%, making it competitive with the more mature $Cu(In,Ga)Se_2$ based technologies. We study the compositional dependence of the physical properties of CZTSSe alloys through first-principles calculations and find that, these mixed-anion alloys are highly miscible with low enthalpies of formation, and the cations maintain the same ordering preferences as the parent compounds Cu_2ZnSnS_4 and $Cu_2ZnSnSe_4$. The band gap of the CZTSSe alloy decreases with the Se content almost linearly, and the band alignment between Cu_2ZnSnS_4 and $Cu_2ZnSnSe_4$ is of type-I, which allows for more facile n-type and p-type doping for alloys with high Se content. Based on these results we analyze the influence of composition on the efficiency of CZTSSe solar cells and explain the high efficiency of the cells with high Se content.

PACS numbers: 61.50.Ah, 71.20.Nr, 71.55.Ht, 72.40.+w

I. INTRODUCTION

Kesterite structured Cu_2ZnSnS_4 (CZTS) is a promising semiconductor for low-cost and sustainable thin-film solar cell devices.[1–7] All of the constituent elements of CZTS are naturally abundant and the band gap is close to the optimal single-junction value (∼1.5 eV).[8] Recently the alloy of CZTS and its Se counterpart $Cu_2ZnSnSe_4$ (CZTSe), which adopts the same crystal structure but has a smaller band gap (∼ 1.0 eV)[9,10,12–14] has generated interest: $Cu_2ZnSn(S,Se)_4$ (CZTSSe) has been used as a solar cell absorber,[15,16] with a light to electricity conversion efficiency as high as 10%,[17] making it competitive with the more mature $Cu(In,Ga)Se_2$ based thin film solar cells.

One well-known limitation for $Cu(In,Ga)Se_2$ solar cells is that the maximum efficiency is achieved by the alloys with low Ga content and band gap (∼1.15 eV), rather than those with high Ga content where the band gap is optimal according to the Shockley-Queisser model.[8] The influence of composition on the solar cell performance is related to the structural, electronic and defect properties of the alloys, such as the In−Ga inhomogeneity,[18] the difficultly of n-type doping, and deep defect levels in the alloys with high Ga content.[19–21] As we develop CZTSSe based solar cells, one natural question arises: is there a similar limit to the efficiency as in $Cu(In,Ga)Se_2$ cells, and why the current highest-efficiency solar cell is based on the alloy with high Se content rather than with high S content which should have a more optimal band gap? To answer this question, a clear understanding of the structural and electronic property dependence on the composition of the $Cu_2ZnSn(S,Se)_4$ alloys is necessary. However, although recent studies have addressed the structural, electronic and defect properties of the parent CZTS and CZTSe,[9,10,22–24] there is no detailed understanding of the CZTSSe alloy.

In this paper, we use the special quasi-random structure (SQS) method to describe the random occupation of S and Se at the anion sites of the CZTSSe alloy,[25,26] and study the compositional dependence of the physical properties through first-principles calculations within density functional theory (DFT). We find that these mixed-anion alloys are highly miscible, with low enthalpies of formation superior to the $Cu(In,Ga)Se_2$ alloys, and that the ground-state cation ordering is the same as the parent compounds, i.e., they adopt the kesterite configuration. The band gap of the CZTSSe alloys decreases with the Se content almost linearly, with a small band gap bowing parameter, and the band alignment between CZTS and CZTSe is of type-I, which allows for more facile n-type and p-type doping for alloys with high Se content. Based on these results we analyze the influence of composition on the efficiency of CZTSSe solar cells and explain the high efficiency of the cells with high Se content.

II. CALCULATION METHODS

The total energy and band structure were calculated within the density functional formalism as implemented in the VASP code.[34] For the exchange-correlation potential, we used the generalized gradient approximation (GGA)

of Perdew and Wang, known as PW91[35]. Since the semi-local GGA usually underestimates the band gap of semiconductors significantly, we also calculate the band gaps employing a more sophisticated hybrid functional, the HSE (Heyd-Scuseria-Ernzerhof) functional in which one quarter of Hartree-Fock non-local exchange interaction is added to the GGA functional, and a screening of μ=0.2 $\AA^{-1}$ is applied to partition the exchange potential into short-range and long-range terms.[36] The d states of group IV elements are treated explicitly as valence. The interaction between the core electrons and the valence electrons is included by the frozen-core projector augmented-wave method,[37] and an energy cut-off of 300 eV was applied for the plane-wave basis set. A 2×2×2 Monkhorst-Pack k-point mesh[38] is used for the Brillouin-zone integration of the 64-atom SQS cell. The convergence test shows the increase of energy cut-off and k-points change the band gap by less than 0.01 eV and the alloy formation energy by less than 0.1 meV/atom. All lattice vectors and atomic positions were fully relaxed by minimizing the quantum mechanical stresses and forces.

The band alignment between different semiconductors is calculated following the same procedure as in the core-level photoemission measurements, and the methods have been described in detail in References.[26,32,39]. It should be mentioned that the method involves the calculation of superlattice structures between different semiconductors, thus the calculated band offset is dependent on the orientation of the superlattice, but the difference is small if the local charge-neutrality condition is satisfied and the charge transfer across the interface is not significant in the superlattice. For the zinc-blende, and zinc-blende-derived chalcopyrite and kesterite semiconductors studied in this paper, a (001) superlattice is used for the band offset calculation, and our test shows that the valence band offsets calculated using the non-equivalent (001) and (100) superlattices differ by less than 0.05 eV, at the order of the calculation error of this method,[11,39] showing that the dependence on the superlattice orientation is not significant for these systems.

III. MIXING ENTHALPY

As we know, pure CZTS and CZTSe are most stable in the zinc-blende-derived kesterite structure, with all cations in one face-centered-cubic sublattice and all anions in another.[9,10,22] Therefore, we may expect that in the random alloy, $Cu_2ZnSn(S_{1-x}Se_x)_4$, the cations will keep the same ordering as in kesterite, while the S and Se anions will be randomly distributed in their sublattice. To mimic the random distribution of S and Se anions, we employ the SQS approach with a 64-atom supercell.[25,26] The SQS for $Cu_2ZnSn(S_{1-x}Se_x)_4$ at $x = 0.25$ is plotted in Figure 1, in which all cations are ordered in the kesterite structure, and the occupation of anions is generated so that the pair-correlation function is closest to that of the random alloy. The occupation of anions at different composition $x = 0.25$, 0.5 and 0.75 are listed in Table. I of Ref. 26.

The enthalpy of mixing for alloy formation is defined as:

$$\Delta H(x) = E(x) - (1-x)E_{CZTS} - xE_{CZTSe}, \tag{1}$$

where E_{CZTS} and E_{CZTSe} represent the total energy of pure CZTS and CZTSe in the kesterite structure, and $E(x)$ is the total energy of the alloy for composition x. In Figure 2, the black circles show the calculated formation enthalpy of the $Cu_2ZnSn(S_{1-x}Se_x)_4$ alloy for x=0.25, 0.5 and 0.75, in which the cations are ordered as in the kesterite structure. As we can see, the formation enthalpy is positive, i.e., the alloy prefers phase segregation into CZTS and CZTSe at zero temperature, and it costs additional energy to mix S and Se anions to form the random alloy. Usually the enthalpy of alloy formation obeys the following relation with content x:

$$\Delta H(x) = (1-x)\Delta H(0) + x\Delta H(1) + \Omega x(1-x), \tag{2}$$

where Ω is the interaction parameter that describes the cost of mixing. In Figure 2, the black line shows the results for kesterite ordering with a fitted interaction parameter of $\Omega = 26$ meV/atom (or 52 meV/mixed-atom). Applying mean-field theory to the free energy of the solid-solution, we estimate that the miscibility temperature is less than 300 K, suggesting that the system is stable at typical growth temperatures. This result is at variance with that for $Cu(In_xGa_{1-x})Se_2$ (CIGS) alloys, where the interaction parameter is about 176 meV/mixed-atom,[27] so phase separation and alloy inhomogeneity are common problems for the production of CIGS based solar cells.[18]

In the above discussion, we have assumed that the cations in $Cu_2ZnSn(S_{1-x}Se_x)_4$ alloys are ordered as in the kesterite structure; however, in pure CZTS and CZTSe the cations may also adopt a partially (Cu+Zn) disordered kesterite structure or the stannite structure.[9,28] To assess the stability of these configurations, we have also calculated the properties of the alternative orderings within the SQS method. The calculated enthalpies of formation are plotted in Figure 2. Note that the energy of the metastable structures is higher than that of kesterite for pure CZTS and CZTSe, so the formation enthalpy at $x = 0$ and 1 is not zero. The relative structural stability is kept for alloys at all compositions over $0 < x < 1$, i.e., the energy increases in the order: kesterite, disordered kesterite and stannite. Furthermore, the energy differences between these structures are kept almost constant at different compositions, e.g., 3-4 meV/atom between stannite and kesterite, and ∼0.3 meV/atom between the partially disordered kesterite and

kesterite. The small energy differences, especially for the partially disordered kesterite, indicate that these alternative configurations are likely to coexist in the synthesized alloy.

IV. BAND GAP BOWING

With knowledge of the alloy structure, we will now address the electronic trends. The band gap changes for the random alloys at each composition are plotted in Figure 3 at two levels of theory. The top panel shows the results from the semi-local GGA functional and the bottom panel shows the results from non-local HSE functional. It should be noted that the GGA underestimates the band gap, and even gives negative values at large x, which means that the conduction band minimum (CBM) Γ_{1c} state is below the valence band maximum (VBM) Γ_{4v} state.[26,28] Relative to the GGA, HSE gives more quantitative band gap values, 1.5 eV at $x = 0$ and 0.96 eV at $x = 1$, which agrees with recent experimental measurements.[12,29]

As shown in Figure 3, the alloy band gap decreases monotonically when the Se content increases, from 1.5 eV at x=0 to 0.96 eV at x=1. The decrease is almost linear, i.e., the band gap bowing parameter, defined from:

$$E_g(x) = xE_g(CZTS) + (1-x)E_g(CZTSe) - bx(1-x), \tag{3}$$

is small ($b \sim 0.1$ eV) and compositionally independent. The bowing values are similar at both levels of theory, indicating that the band gap error for the GGA functional is systematically canceled (see Eq. 3) so that the bowing parameter is correctly reproduced. The calculated band gap bowing of $Cu_2ZnSn(S_{1-x}Se_x)_4$ is similar to that found for $CuGa(S_{1-x}Se_x)_2$ (0.07 eV[26]) and $CuIn(S_{1-x}Se_x)_2$ (0.04 eV[27]) alloys. The small bowing of these mixed anion alloys is because S and Se have small size and chemical difference.[27]

V. BAND ALIGNMENT

To demonstrate how the band gap decreases from CZTS to CZTSe, i.e., the contribution from the valence and conduction bands, we have also calculated the band offset using a well-defined computational procedure.[26,30] As shown in Figure 4, the band alignment between CZTSe and CZTS is of type-I, that is, the valence band is higher and the conduction band is lower at the CZTSe side compared to CZTS, so both electron and hole states will be localized on CZTSe when an interface is formed between the two materials.

This band alignment can be understood according to the nature of the VBM and CBM states: (i) for Cu based chalcogenides including the quaternary Cu_2ZnSnS_4, $Cu_2ZnSnSe_4$ and ternary $CuInSe_2$, $CuGaSe_2$ compounds, the VBM is an antibonding state of the anion p and Cu d orbitals.[26,28] The S p level is lower than Se, thus the VBM of the sulfides is lower than that of the selenides, e.g. the VBM is 0.52 eV lower for ZnS than ZnSe,[30] but the difference is reduced by $p-d$ hybridization in Cu based chalcogenides, because the hybridization is stronger in the shorter Cu-S bond, and pushes the antibonding VBM level of the Cu based sulfide up relative to that of the selenide. As a result, the valence band offset between Cu_2ZnSnS_4 and $Cu_2ZnSnSe_4$ is only 0.15 eV, and a similarly small offsets exists between $CuGaS_2$ and $CuGaSe_2$, and $CuInS_2$ and $CuInSe_2$. Since the $p-d$ hybridization is similar for all Cu based selenides, the valence band offsets are smaller, as shown in Figure 4. (ii) The CBM of Cu_2ZnSnS_4 and $Cu_2ZnSnSe_4$ is the antibonding state of the anion s and Sn s orbitals. Although the s level of S is 0.2 eV lower in energy than Se, the shorter bond length of Sn-S makes the level repulsion stronger in Cu_2ZnSnS_4 and moves its CBM up relative to $Cu_2ZnSnSe_4$.

The conduction band offset (0.35 eV) is larger than the valence band offset (0.15 eV), so it is expected that as the Se content increases in the $Cu_2ZnSn(S_{1-x}Se_x)_4$ alloy, the CBM down-shift plays a more important role than the VBM up-shift for band gap reduction. As the band gap bowing is small, it is expected that the shift of band edge states is linear as a function of the composition x. Considering that the band component of the top valence and bottom conduction band is similar for CZTS and CZTSe, their frequency dependence of the optical transition matrix and adsorption coefficients should be comparable. Previous calculation of the adsorption spectrum supports this analysis, and the main difference between the spectrums of CZTS and CZTSe is an energy shift in the onset to absorption, i.e., the band-gap energy.[10] For the same reason, the optical adsorption spectrums of $Cu_2ZnSn(S_{1-x}Se_x)_4$ alloys should be similar to those of CZTS and CZTSe, and the linear shift of the band edge states as a function of the composition indicates that the absorption spectrum shifts linearly to lower energy side as the composition x increases and the band gap decreases.

Now we will analyze the influence of the band edge shifts with Se content on the doping properties of CZTSSe alloys. According to the doping limit rules, a semiconductor is difficult to be doped n-type if the conduction band level is

too high, and is difficult to be doped p-type if the valence band is too low in energy.[31] For n-type doping of I-III-VI_2 chalcopyrites, it has been shown that the Fermi energy level is pinned at about 0.06 eV above the CBM of $CuInSe_2$, indicating that a I-III-VI_2 semiconductor will be difficult to be doped to n-type if its CBM level is much higher than this pinning level. Since kesterite Cu_2ZnSnS_4 and $Cu_2ZnSnSe_4$ have a similar electronic structure to that of $CuInSe_2$, we can assume that the Fermi energy pinning level lines up for all chalcopyrite and kesterite compounds.[31] In Figure 4, the red dashed line shows this pinning level. We can see that the line falls below the CBM level of Cu_2ZnSnS_4, while above that of $Cu_2ZnSnSe_4$, which indicates that the later is relatively easier to be doped to n-type.

It is well known that for CIGS solar cells, the efficiency approaches a maximum at low Ga content and starts to decrease if the Ga concentration is further increased, although the band gap becomes closer to the optimal gap value of ∼1.5 eV. One of the origins for this behavior has been attributed to the fact that $CuInSe_2$ can be easily doped n-type and thus can exhibit a type-inverted n-type phase at the surface of the p-type absorber, which facilitates electron-hole separation of photogenerated carriers. However, $CuGaSe_2$ is difficult to be doped n-type and thus $Cu(In_xGa_{1-x})Se_2$ alloys with high Ga concentration exhibit lower conversion efficiency.[19,20] Based on the same argument, we expect that solar cells based on $Cu_2ZnSn(S_{1-x}Se_x)_4$ alloys with high Se concentration will have higher efficiency than those with low Se content because the former can be converted more easily to n-type. This may explain why currently the highest solar cell efficiency is achieved for alloys with high Se concentration,[17] which have lower than optimal band gaps.

The p-type doping, or self-doping, is related mainly to the electronic states near the top of the valence band. Defect analysis for Cu_2ZnSnS_4 has shown that the facile formation of defects such as the Cu_{Zn} antisite and Cu vacancy make it p-type intrinsically, but the ionization level of the dominant Cu_{Zn} antisite is relatively deeper than that of the Cu vacancy.[32] This acceptor level will limit the generation of free-carriers in the absorber layer of the photovoltaic device. The deep level originates from strong $p-d$ hybridization between Cu and S. In $Cu_2ZnSnSe_4$ the $p-d$ hybridization is weaker and the valence band is higher, thus we expect that the ionization level of the Cu_{Zn} antisite should be shallower as the Se concentration increases in $Cu_2ZnSn(S_{1-x}Se_x)_4$ alloys, which is an important factor for the solar cell performance.

In Figure 4 we also show the band alignment between Cu_2ZnSnS_4, $Cu_2ZnSnSe_4$ and CdS which is the common n-type window layer used to form the p-n junction with the p-type absorber. For the device design, type-II band alignment between the window and absorber layer could be beneficial to facilitate electron-hole separation. Since the CBM level of CdS is between those of Cu_2ZnSnS_4 and $Cu_2ZnSnSe_4$, there is a type-II to type-I conversion as the Se concentration increases in the CZSSe alloy. In this regard, alloys with high Se concentration may not be optimal. It should be noted that CIGS alloys with high In content also have type-I alignment relative to CdS, but it is changed to type-II by the internal electric field formed in the p-n junction, according to device simulation.[33] We therefore expect that this factor is not a major concern in $Cu_2ZnSn(S_{1-x}Se_x)_4$ based solar cells.

VI. CONCLUSION

In conclusion, we have investigated the properties of $Cu_2ZnSn(S_{1-x}Se_x)_4$ as a function of the alloy composition x. The calculated enthalpy of formation shows that the mixed-anion alloys are highly miscible, and that the cations maintain the same ordering preferences as in pure kesterite structured Cu_2ZnSnS_4 and $Cu_2ZnSnSe_4$. Partial cation disorder is, however, still possible due to the low energetic cost. The band gaps of the random alloy decrease with Se content. There is a small bowing parameter, and the conduction band down-shift contributes more to the gap decrease than the valence band up-shift. The band alignment between Cu_2ZnSnS_4 and $Cu_2ZnSnSe_4$ is of type-I. The lower conduction band makes the $Cu_2ZnSn(S,Se)_4$ alloys with high Se concentration easier to be doped n-type, while the higher valence band makes the ionization level of the dominant p-type defect shallower. The balance between the band gap size and the doping ability will determine the optimal alloy composition to achieve high efficiency $Cu_2ZnSn(S_{1-x}Se_x)_4$ based solar cells.

VII. ACKNOWLEDGMENTS

The work in Fudan is supported by the Natural Sciences Foundation (NSF) of China (10934002, 1095011032), the Research Program of Shanghai municipality and MOE, the Special Funds for Major State Basic Research. The work in ECNU is supported by NSF of Shanghai (10ZR1408800) and China (61076060) and the Fundamental Research Funds for the Central Universities. A.W. would like to acknowledge funding of a Marie-Curie Fellowship from the European Union and an International Young Scientist Fellowship from NSF of China (10950110324). The work at NREL is funded by the U.S. Department of Energy, under Contract No. DE-AC36-08GO28308.

[1] Q. Guo, H. W. Hillhouse, and R. Agrawal, J. Am. Chem. Soc. **131**, 11672 (2009).
[2] A. Weber, S. Schmidt, D. Abou-Ras, P. Schubert-Bischoff, I. Denks, R. Mainz, and H. W. Schock, Appl. Phys. Lett. **95**, 041904 (2009).
[3] J. J. Scragg, P. J. Dale, L. M. Peter, G. Zoppi, and I. Forbes, Phys. Status Solidi B **245**, 1772 (2008).
[4] H. Katagiri, K. Jimbo, W. S. Maw, K. Oishi, M. Yamazaki, H. Araki, and A. Takeuchi, Thin Solid Films **517**, 2455 (2009).
[5] Y. K. Kumar, G. S. Babu, P. U. Bhaskar, and V. S. Raja, Solar Energy Materials and Solar Cells **93**, 1230 (2009).
[6] A. Weber, H. Krauth, S. Perlt, B. Schubert, I. Kötschau, S. Schorr, and H. Schock, Thin Solid Films **517**, 2524 (2009).
[7] K. Wang, O. Gunawan, T. Todorov, B. Shin, S. J. Chey, N. A. Bojarczuk, D. Mitzi, and S. Guha, Appl. Phys. Lett. **97**, 143508 (2010).
[8] W. Shockley and H. J. Queisser, J. Appl. Phys. **32**, 510 (1961).
[9] S. Chen, X. G. Gong, A. Walsh, and S.-H. Wei, Appl. Phys. Lett. **94**, 041903 (2009).
[10] C. Perrson, J. Appl. Phys. **107**, 053710 (2010).
[11] S.-H. Wei and A. Zunger, Appl. Phys. Lett. **63**, 2549 (1993).
[12] S. Ahn, S. Jung, J. Gwak, A. Cho, K. Shin, K. Yoon, D. Park, H. Cheong, and J. H. Yun, Appl. Phys. Lett. **97**, 021905 (2010).
[13] A. Shavel, J. Arbiol, and A. Cabot, J. Am. Chem. Soc. **132**, 4514 (2010).
[14] A. Redingera and S. Siebentritt, Appl. Phys. Lett. **97**, 092111 (2010).
[15] M. Altosaar, J. Raudoja, K. Timmo, M. Danilson, M. Grossberg, J. Krustok, and E. Mellikov, Phys. Status Solidi A **205**, 167 (2008).
[16] J. Krustok, R. Josepson, M. Danilson, and D. Meissner, Solar Energy **84**, 379 (2010).
[17] T. K. Todorov, K. B. Reuter, and D. B. Mitzi, Adv. Mater. **22**, E156 (2010).
[18] C. D. R. Ludwig, T. Gruhn, C. Felser, T. Schilling, J. Windeln, and P. Kratzer, Phys. Rev. Lett. **105**, 025702 (2010).
[19] C. Persson, Y.-J. Zhao, S. Lany, and A. Zunger, Phys. Rev. B **72**, 035211 (2005).
[20] S.-H. Wei and S. B. Zhang, J. Phys. Chem. Solids **66**, 1994 (2005).
[21] S. Lany and A. Zunger, Phys. Rev. Lett. **100**, 016401 (2008).
[22] J. Paier, R. Asahi, A. Nagoya, and G. Kresse, Phys. Rev. B **79**, 115126 (2009).
[23] A. Nagoya, R. Asahi, R. Wahl, and G. Kresse, Phys. Rev. B **81**, 113202 (2010).
[24] S. Chen, X. G. Gong, A. Walsh, and S.-H. Wei, Appl. Phys. Lett. **96**, 021902 (2010).
[25] S.-H. Wei, L. G. Ferreira, J. E. Bernard, and A. Zunger, Phys. Rev. B **42**, 9622 (1990).
[26] S. Chen, X. G. Gong, and S.-H. Wei, Phys. Rev. B **75**, 205209 (2007).
[27] S.-H. Wei and A. Zunger, J. Appl. Phys. **78**, 3846 (1995).
[28] S. Chen, X. G. Gong, A. Walsh, and S.-H. Wei, Phys. Rev. B **79**, 165211 (2009).
[29] G. S. Babu, Y. K. Kumar, P. U. Bhaskar, and V. S. Raja, Semicond. Sci. Technol. **23**, 085023 (2008).
[30] Y.-H. Li, A. Walsh, S. Chen, W.-J. Yin, J.-H. Yang, J. Li, J. L. F. D. Silva, X. G. Gong, and S.-H. Wei, Appl. Phys. Lett. **94**, 212109 (2009).
[31] S. B. Zhang, S.-H. Wei, and A. Zunger, J. Appl. Phys. **83**, 3192 (1998).
[32] S. Chen, J.-H. Yang, X. G. Gong, A. Walsh, and S.-H. Wei, Phys. Rev. B **81**, 245204 (2010).
[33] M. Gloeckler and J. Sites, Thin Solid Films **480-481**, 241 (2005).
[34] G. Kresse and J. Furthmuller, Phys. Rev. B **54**, 11169 (1996).
[35] J. P. Perdew, J. A. Chevary, S. H. Vosko, K. A. Jackson, M. R. Pederson, D. J. Singh, and C. Fiolhais, Phys. Rev. B **46**, 6671 (1992).
[36] J. Heyd, G. E. Scuseria, and M. Ernzerhof, J. Chem. Phys. **118**, 8207 (2003).
[37] G. Kresse and D. Joubert, Phys. Rev. B **59**, 1758 (1999).
[38] H. J. Monkhorst and J. D. Pack, Phys. Rev. B. **13**, 5188 (1976).
[39] S.-H. Wei and A. Zunger, Appl. Phys. Lett. **72**, 2011 (1998).

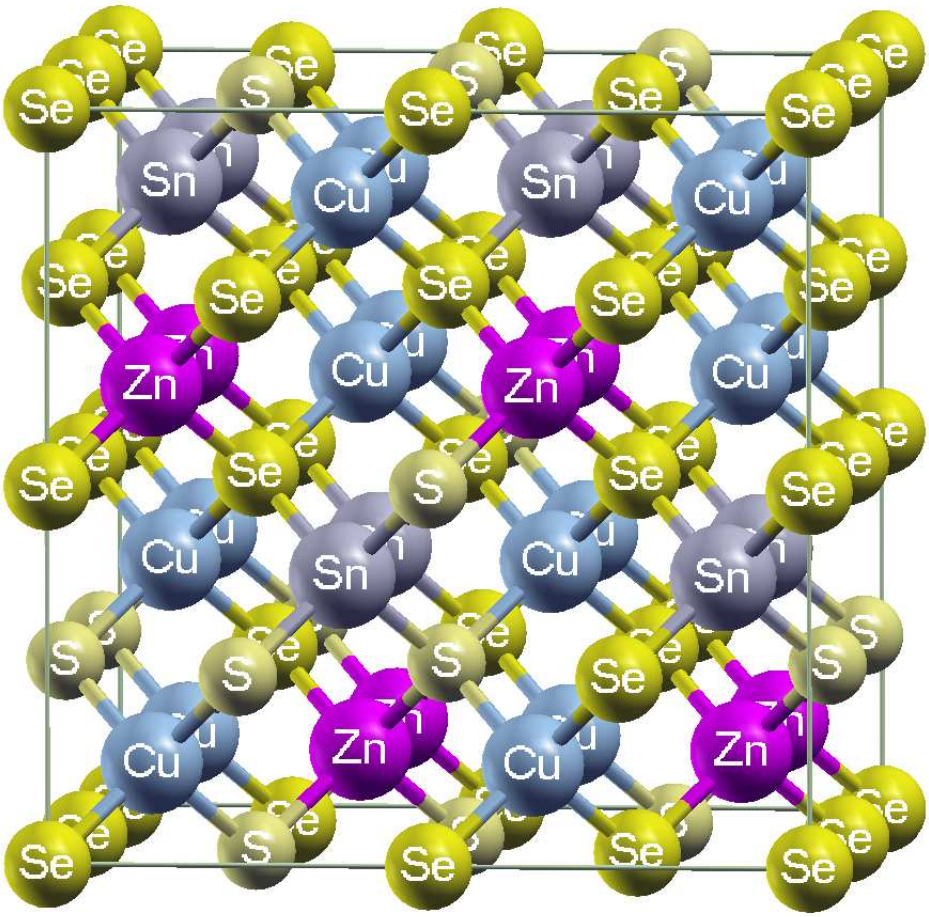

FIG. 1: (Color online) The special quasirandom structure of $Cu_2ZnSn(S_{0.25}Se_{0.75})_4$ with cations ordered in the kesterite structure.

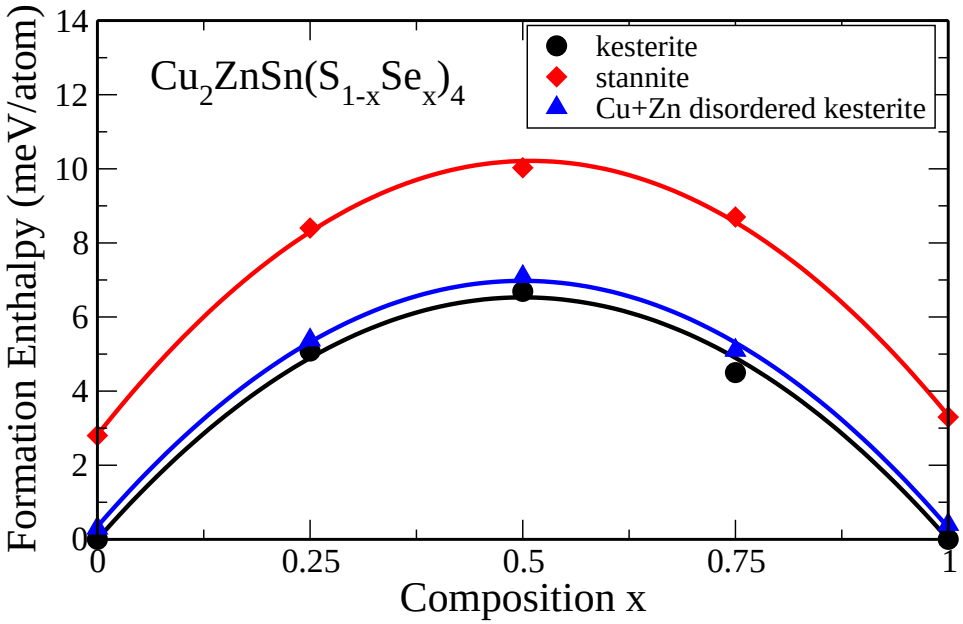

FIG. 2: (Color online) The calculated enthalpy of formation for the $Cu_2ZnSn(S_{1-x}Se_x)_4$ alloy as a function of alloy composition x and cation ordering, relative to phase-separated kesterite Cu_2ZnSnS_4 and $Cu_2ZnSnSe_4$.

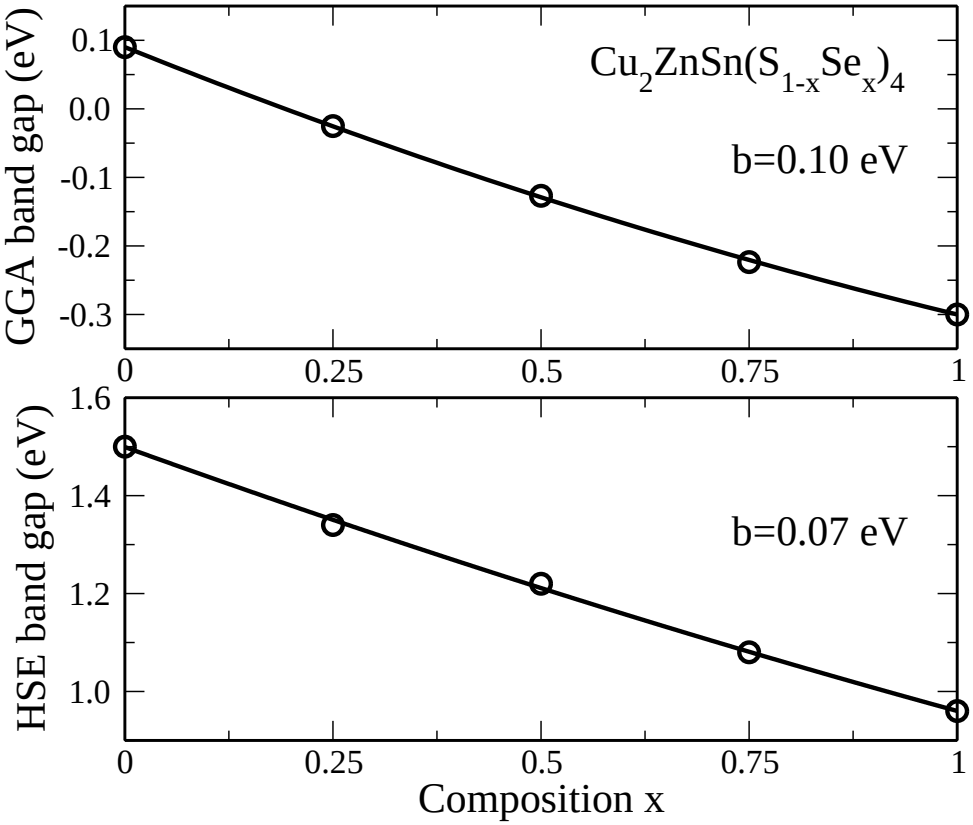

FIG. 3: The calculated band gap of $Cu_2ZnSn(S_{1-x}Se_x)_4$ at different composition (x) using the GGA functional (top panel) and HSE functional (bottom panel).

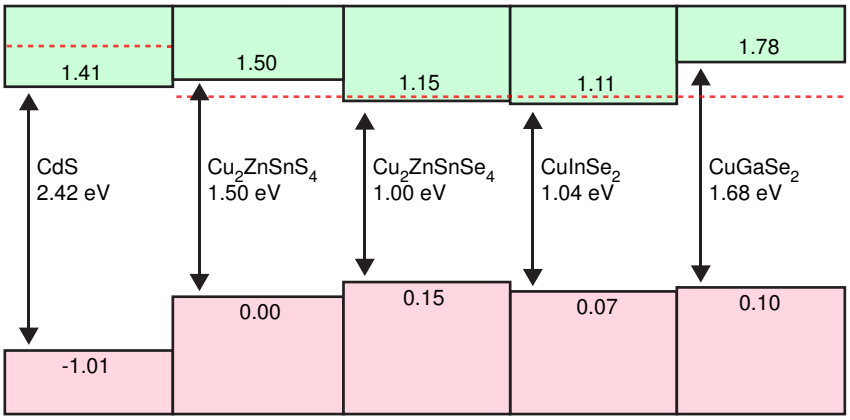

FIG. 4: (Color online) The band alignment between CdS, Cu_2ZnSnS_4, $Cu_2ZnSnSe_4$, $CuInSe_2$ and $CuGaSe_2$ (the effects of spin-orbit coupling are included). The red (dashed) line near the conduction band shows the pinning energy of Fermi level for n-type doping.